Ecotoxicology and Environmental Safety 239 (2022) 113623

Contents lists available at ScienceDirect

Ecotoxicology and Environmental Safety

journal homepage: www.elsevier.com/locate/ecoenv

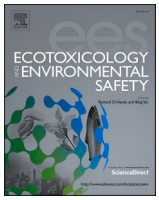

Effects of Bisphenol A on reproductive toxicity and gut microbiota dysbiosis in male rats

Ruijing Liu [a], Dongbao Cai [b], Xusheng Li [b], Boping Liu [a], Jiali Chen [b], Xinwei Jiang [b], Haiwei Li [b], Zhenhua Li [c], Katja Teerds [d], Jianxia Sun [e], Weibin Bai [b,*], Yulong Jin [a,**]

[a] Key Laboratory for Bio-Based Materials and Energy of Ministry of Education, College of Materials and Energy, South China Agricultural University, Guangzhou 510630, PR China
[b] Department of Food Science and Engineering, Institute of Food Safety and Nutrition, Guangdong Engineering Technology Center of Food Safety Molecular Rapid Detection, Jinan University, Guangzhou 510632, PR China
[c] Zhuhai Precision Medical Center, Zhuhai People's Hospital (Zhuhai Hospital Affiliated with Jinan University), Jinan University, Zhuhai 519070, PR China
[d] Department of Animal Sciences, Human and Animal Physiology, Wageningen University, Wageningen, The Netherlands
[e] School of Chemical Engineering and Light Industry, Guangdong University of Technology, Guangzhou 510006, PR China

ARTICLE INFO

Edited by Dr Yong Liang

Keywords:
Bisphenol A
Male reproduction
Hormone
Mammalian target of rapamycin
Apoptosis
Gut microbiota

ABSTRACT

Bisphenol A (BPA) is an environmental endocrine disruptor. Recent studies have shown an association between decreased spermatogenesis and gut microbiota alteration. However, the potential associations and mechanisms of BPA exposure on spermatogenesis, hormone production, and gut microbiota remain unknown. This study aims to investigate BPA-induced male reproductive toxicity and the potential link with gut microbiota dysbiosis. Male Sprague Dawley rats were exposed to BPA at different doses by oral gavage for thirty consecutive days. The extent of testicular damage was evaluated by basic parameters of body weight and hematoxylin-eosin (H&E) staining. Next, we determined the mRNA levels and protein levels of apoptosis, histone-related factors, and mammalian target of rapamycin (mTOR) pathway in testes. Finally, 16 S rDNA sequencing was used to analyze gut microbiota composition after BPA exposure. BPA exposure damaged testicular histology, significantly decreased sperm count, and increased sperm abnormalities. In addition, BPA exposure caused oxidative stress and cell apoptosis in testes. The levels of histone (H2A, H3) were significantly increased, while ubiquitin histone H2A (ub-H2A) and ubiquitin histone H2B (ub-H2B) were markedly reduced. Furthermore, BPA activated the PI3K and AKT expression, but the protein expressions of mTOR and 4EBP1 in testes were inhibited significantly. Additionally, the relative abundance of class Gammaproteobacteria, and order Betaproteobacteriales was significantly higher when treated with a high dose of BPA compared to the control group, which was negatively correlated with testosterone level. This study highlights the relationship between BPA-induced reproductive toxicity and gut microbiota disorder and provides new insights into the prevention and treatment of BPA-induced reproductive damage.

Abbreviations: BPA, Bisphenol A; NOAEL, No observed adverse effect level; LOAEL, Lowest observed adverse effect level; PI3K, Phosphoinositide 3-kinase; mTOR, Mammalian target of rapamycin; 4EBP1, 4E-binding protein 1; EDC, Endocrine-disrupting chemical; LH, Luteinizing hormone; FSH, Follicle-stimulating hormone; DHT, Dihydrotestosterone; INHB, Inhibin B; E2, Estradiol; GnRH, Gonadotrophin-releasing hormone; HPG, Hypothalamic-pituitary-gonadal; EE, Ethinyl estradiol; Bax, Bcl-2-associated X protein; Bcl-2, B-cell lymphoma 2; TUNEL, Terminal deoxynucleotidyl transferase-mediated nick end labeling; eIF4E, Eukaryotic translation initiation factor 4E; PARP, Poly (ADP-ribose) polymerase; Raptor, Regulatory-associated protein of mTOR; SOD, Superoxide dismutase; GSH, Glutathione; CAT, Catalase; MDA, Malondialdehyde; GPR54, G protein-coupled receptor 54; BTB, Blood-testis barrier.

* Correspondence to: Department of Food Science and Engineering, Institute of Food Safety and Nutrition, Jinan University, 601 Huangpu Rd, Guangzhou 510632, PR China.
** Corresponding author.
E-mail addresses: baiweibin@163.com (W. Bai), jyl@scau.edu.cn (Y. Jin).

https://doi.org/10.1016/j.ecoenv.2022.113623
Received 12 March 2022; Received in revised form 23 April 2022; Accepted 7 May 2022
Available online 11 May 2022

1. Introduction

Bisphenol A (BPA), a known endocrine-disrupting chemical (EDC) with estrogenic activity, is a synthetic chemical that is found in large quantities in the environment (Liu et al., 2021b; Molina et al., 2018). It is widely used to produce polycarbonate plastics, epoxy resin liners for food cans, water bottles, some dental sealants and composites, thermal receipts, and other applications (Ehrlich et al., 2014). BPA can migrate into the water and food under conditions such as high temperature, acidity, and alkalinity (Vandenberg et al., 2009). The routes of human exposure to BPA are various including inhalation (dust, occupational sources) and dermal contact (household products, cosmetics, medical devices) (Cho et al., 2012; Demierre et al., 2012; Buckley et al., 2019). Data from a national survey showed that about 90% of the general population in Canada had detectable urinary BPA levels (>0.2 ng/mL) (Health Canada, 2015), and in the US this percentage is even higher (92.6%) (Calafat et al., 2008). BPA exposure is associated with a variety of health problems, especially male reproductive disorders. Sing et al. reported a reduction in the percentage of live sperm and a concomitant increase in the percentage of dead sperm after exposure to different doses of BPA (Singh et al., 2015). Analysis of testicular histology revealed that in ICR mice pups postnatal BPA exposure led to a block in the progression of meiosis and an increase in germ cell apoptosis during the first wave of spermatogenesis (Xie et al., 2016). Moreover, paternal BPA exposure in CD-1 mice affected spermatogenesis by decreasing the number stage of VIII seminiferous epithelial cells, causing a decline in total sperm counts and sperm motility in the F1 offspring (Rahman and Pang, 2019).

In males, spermatogenesis is a highly complicated process involving mitosis of spermatogonia, meiosis of spermatocytes, and the differentiation of round spermatids into mature sperm (Liu et al., 2021a). The main regulators of spermatogenesis are the gonadotropic hormones luteinizing hormone (LH) and follicle-stimulating hormone (FSH) which are released by the pituitary in response to the hypothalamic derived releasing neurohormone gonadotrophin-releasing hormone (GnRH) (Corradi et al., 2016; Qiu et al., 2018). Furthermore, testosterone synthesis in Leydig cells was mainly controlled by luteinizing hormone (LH), which together with FSH regulates Sertoli cell function and the normal progression of spermatogenesis within the seminiferous tubules (Spaziani et al., 2021). Kisspeptin neurons in the hypothalamus act to regulate the activity of GnRH neurons and thus, in turn, the downstream hypothalamic-pituitary-gonadal (HPG) endocrine axis (Abbara et al., 2021). The GnRH neurons in the hypothalamus are however not directly able to respond to fluctuations in circulating testosterone levels but respond to changes in kisspeptin release, a neurotransmitter that binds to the GPR54 receptor on the GnRH neurons. Kisspeptin is produced by the kisspeptin neurons in the hypothalamus which express androgen receptors and thus can respond via a negative feedback mechanism, to changes in circulating testosterone levels (Poling and Kauffman, 2013). BPA was able to bind androgen receptors (AR) and acted as an androgen antagonist to block the effect of endogenous androgens, thereby affecting the transmission of hormone signals in target cells, tissues, and organs, resulting in the corresponding biological effects, and then causing dysfunction of the reproductive system of the body (Murata and Kang, 2018).

In addition, the histone-to-protamine exchange is the first step during post-meiotic male germ cell development, when haploid round spermatids elongate and transform into spermatozoa. The failure of histone-to-protamine exchange may contribute to male sterility (Gou et al., 2017). The mammalian target of rapamycin (mTOR), belonging to the phosphatidylinositol kinase-related kinase family, is a serine-threonine protein kinase that is regulated by proline (Xu et al., 2016). Activation of the phosphoinositide 3-kinase/protein kinase B/mTOR (PI3K/AKT/mTOR) signaling pathway initiates the efficient translation of mRNAs required for spermatogonial differentiation. At present, studies investigating the impact of this pathway on testicular function are numerous (Gao et al., 2020; Kong et al., 2021; Ni et al., 2021; Fu et al., 2020).

The intestinal microbiota is a complex ecosystem in humans and animals, and it has been found to play an important role in controlling host health. Modulation of the intricate relationship between the host and microbiome can result in many diseases such as cancer, metabolic, cardiovascular, immune, and neurobehavioral disorders (Diamante et al., 2021). Some exogenous compounds can disrupt gut microbiota composition and induce negative health effects (Zhan et al., 2020). Low-dose exposures to diethyl phthalate, methylparaben, and triclosan decreased the body weight of adolescent rats, which coincides with a decrease in the Firmicutes/Bacteroidetes ratio (Hu et al., 2016). Moreover, BPA is likely to influence organisms via changes in microbial companions. A previous study showed that exposure to BPA increased the abundance of *Lactobacilllus*, *Alcaligenes*, and *Mycobacterium* in the colon (Wang et al., 2018). Dietary exposure to BPA similarly altered the gut microbiota composition as the intake of a diet high in fat and sucrose does (Lai et al., 2016). In addition, BPA and ethinyl estradiol (EE) at doses that have previously been shown to disturb behavior and metabolism in F1 California mice offspring also led to generational and sex-dependent changes in the gut microbiome (Javurek et al., 2016).

Despite the growing number of researches, the underlying mechanisms between BPA-induced reproductive toxicity and gut microbiota are still limited. Therefore, this study aimed to explore the potential link between BPA-induced intestinal flora disturbance and reproductive toxicity, further provided new insight into the comprehensive understanding of the mechanism of reproductive toxicity of BPA.

2. Materials and methods

2.1. Animals and experimental design

Male Sprague-Dawley rats (3–4weeks) were obtained from Beijing HFK Bioscience Co., LTD. The animals were housed under temperature (22–25 °C) and humidity (40%–60%) controlled conditions with a 12 h light/dark cycle. Rats had ad libitum access to chow and water. BPA (analytical purity≥99%, CAS: 80–05–7) was purchased from Sigma-Aldrich (St. Louis, Missouri, US). After a 7-day adaptation period, the rats were randomly divided into four groups (8 rats/group) and treated as follows: control group (corn oil only), BPA-low (BPA-L), -medium (-M), and -high (-H) group (30, 90, and 270 mg/kg·bw BPA dissolved in corn oil, respectively).

The no observed adverse effect level (NOAEL) and the lowest observable adverse effect level (LOAEL) of BPA were 5 mg/kg·bw and 50 mg/kg·bw, respectively. Here, we chose the "low dose" of BPA $\leq$ 50 mg/kg·bw, and the "medium and high-dose" of BPA is the using concentrations $>$ 50 mg/kg bw referring to previous literature (Adegoke et al., 2022; Peretz et al., 2014). BPA was provided to the rats by daily oral gavage for 30 days. The animal experiment was approved by the Animal Care and Protection Committee of Jinan University (Approval No. IACUC-20201027–12) and was performed by the US NIH Guide for the Care and Use of Laboratory Animals (No. 8023, revised in 1978).

At the end of the experiment, all animals were anesthetized by pentobarbital and sacrificed. Blood was collected from the abdominal aorta for further analysis. The testis and epididymis were quickly removed and weighed. The left testis was snap-frozen and stored at − 80 °C until further analysis. The right testis and epididymis were fixed in modified Davidson's fluid (Scientific Phygene) and 4% paraformaldehyde respectively for further histological analysis. The hypothalamus and pituitary were collected, frozen on dry ice, and stored at − 80 °C for RT-qPCR analysis. The testis and epididymis coefficients were calculated in the following way:

$$\text{testis coefficient} = \frac{testis \quad weight(g)}{body \quad weight(g)} \times 100\%$$

$$\text{epididymis coefficient} = \frac{epididymis \quad weight(g)}{body \quad weight(g)} \times 100\%$$

2.2. Sperm analysis

The left cauda epididymis was used for the evaluation of sperm parameters. The cauda epididymis was trimmed of residual adipose tissue, and then put into a culture dish with 10 mL preheated normal saline (37 °C), cut into small pieces to release the stored sperm, and kept at a temperature of 37 °C for 2 min. After that, 10 μL sperm suspension was subjected to analyze the sperm count, and sperm morphology analysis using a computer-aided semen analysis system (CASA, mL-608ZII, Song Jing Tian Lun Biotechnology Co., Ltd.). At least 30 different fields were analyzed for each sample.

2.3. Determination of oxidative stress in serum and testis

To determine oxidative stress in testis tissue, 0.1 g testis tissue, 10% (w/v) was homogenized in PBS buffer (pH 7.4). The homogenate was centrifuged at 1520g for 20 min after which the supernatant was collected. The assay kits for the detection of superoxide dismutase (SOD), glutathione (GSH), catalase (CAT), and malondialdehyde (MDA) were purchased from Nanjing Jiancheng Bioengineering Institute. The protein concentration of the testis samples was determined by bicinchoninic acid (BCA) protein assay kit (Applygen Technologies Inc., China).

2.4. Histological and immunohistochemical analysis of testis and epididymis

The left testes and epididymides were fixed for 24 h at room temperature, dehydrated in graded ethanol and xylene, and embedded in paraffin. The embedded tissues were cut into 4 μm thick sections and stained with hematoxylin-eosin (H&E).

Immunohistochemical analysis of mTOR was performed as described previously (Jiang et al., 2018). In brief, tissue sections were deparaffinized after which antigen retrieval in citrate buffer (pH 6.0) was performed. The next sections were blocked with 3% hydrogen peroxide in methanol for 15 min at room temperature to block endogenous peroxidase activity and washed three times in phosphate-buffered saline (PBS) (pH 7.4). After blocking the nonspecific sites with 3% BSA, PI3K (1:200, Cat# 20584–1-AP, Proteintech), p-AKT (1:250, Cat# ab81283, Abcam), and mTOR (1:1000, Cat# 66888–1-Ig, Proteintech) primary antibodies were applied to the separate sections, and slides were kept overnight at 4 °C respectively. Subsequently, sections were incubated with the secondary antibody for 50 min, followed by DAB staining, and counterstaining with hematoxylin for 3 min mTOR labeling was examined by a microscope (NIKON ECLIPSE E100, Japan) equipped with an imaging system (NIKON DS-U3). To evaluate the amount of cell staining, the images were analyzed using an image analysis software (Image Pro-Plus 6.0, Media Cybernetics, MD, U.S.A.).

2.5. Determination of hormone levels

Dihydrotestosterone (DHT), FSH, LH, estradiol (E2), inhibin B (INHB), testosterone, and testicular fructose levels were measured in serum, while GnRH content was measured in hypothalamic tissue homogenates, using enzyme-linked immunosorbent assay (ELISA) kits. The ELISA kits for GnRH, DHT, FSH, LH, E2, and INHB were purchased from Jiang Lai Biotechnology Co., Ltd. (Shanghai, China). The ELISA kits for testosterone and fructose were purchased from Cusabio (Wuhan, China) and Nanjing Jiancheng Bioengineering Institute (Nanjing, China), respectively. All procedures were carried out according to the manufacturers' instructions.

2.6. Determination of apoptosis rate in testes

Apoptosis of cells in testicular sections was detected using a terminal-deoxynucleotidyl transferase-mediated nick end labeling (TUNEL) staining following the manufacturer's protocols of the assay kit from Beyotime Biotech (Shanghai, China).

2.7. Quantification of mRNA expression

Total RNA from the hypothalamus and testis was extracted using TRIzol reagent (Beyotime Institute of Biotechnology, China) following the manufacturer's protocol. The cDNA used for quantitative RT-PCR was synthesized using the *Evo M-MLV* RT Kit with gDNA Clean for qPCR II AG11711 (Accurate Biotechnology [Hunan] Co., Ltd, China). RT-PCR reactions were carried out employing the Applied Biosystems QuantStudio 6 using the SYBR® Green Premix Pro Taq HS qPCR Kit AG11701 (Accurate Biotechnology [Hunan] Co., Ltd, China) according to the following procedure: initial temperature of 95 °C for 30 s, followed by 5 s at 95 °C (45 cycles) for denaturation and annealing at 55 °C for 30 s. The primers were synthesized by Shanghai Sangon Biological Engineering Co., Ltd (Guangzhou synthesis department). Relative mRNA expression levels were calculated using the $2^{-\Delta\Delta CT}$ method and were normalized with β-actin. The primers sequences used are listed in Table 1.

2.8. Protein expression analysis

Protein extraction and western blot analysis were performed as previously described (Li et al., 2020). In brief, the testis tissues were homogenized in RIPA buffer (Beyotime, China) supplemented with protease inhibitors and phenylmethanesulfonyl fluoride (PMSF), followed by centrifugation at 14,000g for 10 min at 4 °C after which the supernatant was collected. The BCA protein assay kit was used to determine the protein content of the samples. Equal amounts of protein (20 μg) were separated by 8–12% sodium dodecyl sulfate-polyacrylamide gel electrophoresis (SDS-PAGE) and transferred onto polyvinylidene difluoride (PVDF) membranes. Membranes were blocked with 5% skimmed milk at room temperature for 1.5 h and incubated with the primary antibodies overnight at 4 °C. The primary antibodies Bax (1:500, Cat# AF1020), Bcl-2 (1:500, Cat# AF6139), eIF4E (1:500, Cat# AF6110), FAS (1:500, Cat# AF5342), FASL (1:500, Cat# AF0157), Histone H4 (1:500, Cat# AF6355), and β-actin (1:5000, Cat# T0022) were acquired from Affinity Biosciences (USA). Histone H2A (1:5000, Cat# ab177308), Histone H2B (1:1000, Cat# ab52484), Histone H3 (1:1000, Cat# ab176882), and phospho-AKT (1:5000, Cat# ab81283) was purchased from Abcam (Cambridge, UK). Cleaved-PARP (1:1000, Cat# 94885 S), PARP (1:1000, Cat# 9532 T), ub-H2A (1:2000, Cat# 8240 T), ub-H2B (1:1000, Cat# 5546 T), and were obtained from Cell Signaling Technology (Massachusetts, USA). mTOR (1:5000, Cat# 66888–1-Ig), Raptor (1:500, Cat# 20984–1-AP), AKT (1:1000, Cat# 10176–2-AP), and PI3K (1:500, Cat# 20584–1-AP) were purchased from

Table 1
Primers used for RT-PCR.

Genes	Sequences (5'-3')	Accession No.
Kiss-1	Forward: TGCTGCTTCTCCTCTGTGTG Reverse: CCAGGCATTAACGAGTTCCT	NM_181692.1
Gpr54	Forward: GGAACTCACTGGTCATCTTCGT Reverse: GTACGCAGCACAGAAGGAAAGT	NM_023992.2
P13k	Forward: GATGTCTGCGTTAGGGCTTACC Reverse: TCAGCATCATGGAGAACAGGAT	NM_001371300.2
Akt1	Forward: CTCATTCCAGACCCACGAC Reverse: ACAGCCCGAAGTCCGTTA	NM_033230.3
mtor	Forward: AGCCGTTGTTGCAGAGACTT Reverse: CATGGTTCATGGTGTCTTGC	NM_019906.2
β-actin	Forward: CCCATCTATGAGGGTTACGC Reverse: TTTAATGTCACGCACGATTTC	NM_031144.3

Proteintech (Wuhan, China). Then it was followed by incubation with goat anti-rabbit IgG-HRP (1:2000, Cat# 98164 S) (Cell Signaling Technology, USA) or anti-mouse IgG-HRP (1:5000, Cat# 91196 S) (Proteintech, Wuhan, China) at room temperature for 1 h, as described previously (Jiang et al., 2018). ECL reagent was applied to visualize the bands by the Clinx ChemiScope system (Shanghai, China).

2.9. Gut microbiota analysis by 16S rRNA gene sequencing

Fecal samples were after collection stored at − 80 °C until further processing. Total DNA was extracted from the fecal samples using the MagPure Soil DNA LQ Kit (Magen, China) according to the manufacturer's instructions. DNA concentration and quality were assessed by NanoDrop 2000 spectrophotometry (Thermo Fisher Scientific, USA) and agarose gel electrophoresis, respectively. For bacterial diversity analysis, the V3-V4 variable region of the 16 S rRNA genes was amplified using the universal primers 338 F (5′-ACTCCTACGGGAGGCAGCA-3′) and 806 R (5′-GGACTACHVGGGTWTCTAAT-3′). Amplicon quality was visualized using gel electrophoresis. The PCR products were purified using Agencourt AMPure XP beads (Beckman Coulter Co., USA) and quantified using the Qubit dsDNA assay kit (Life Technologies, USA). Purified amplicons were pooled in equimolar concentrations. Sequencing was performed on the Illumina NovaSeq 6000 sequencing platform with the paired-end read of 2 × 250 cycles according to standard protocols (Illumina Inc., San Diego, CA; OE Biotech Company; Shanghai, China).

For bioinformatic analysis paired-end reads were assembled using FLASH (FLASH: fast length adjustment of short reads to improve genome assemblies). Further processing of paired-end reads including quality filtering, removal of mismatched barcodes, and sequences were completed using QIIME version 1.8.0. Clean reads were subjected to primer sequence removal and clustering to generate operational taxonomic units (OTUs) using Vsearch software with a 97% similarity cutoff. All representative reads were annotated and blasted against Silva database Version 132.

2.10. Statistical analysis

Statistical analyses were conducted using SPSS 23.0 (SPSS Inc., Chicago, USA). GraphPad Prism software, version 8.0 (San Diego, USA) and Origin, version 9.1 (OriginLab Corp., Northampton, MA) were used for figure design. A significant difference was determined by one-way

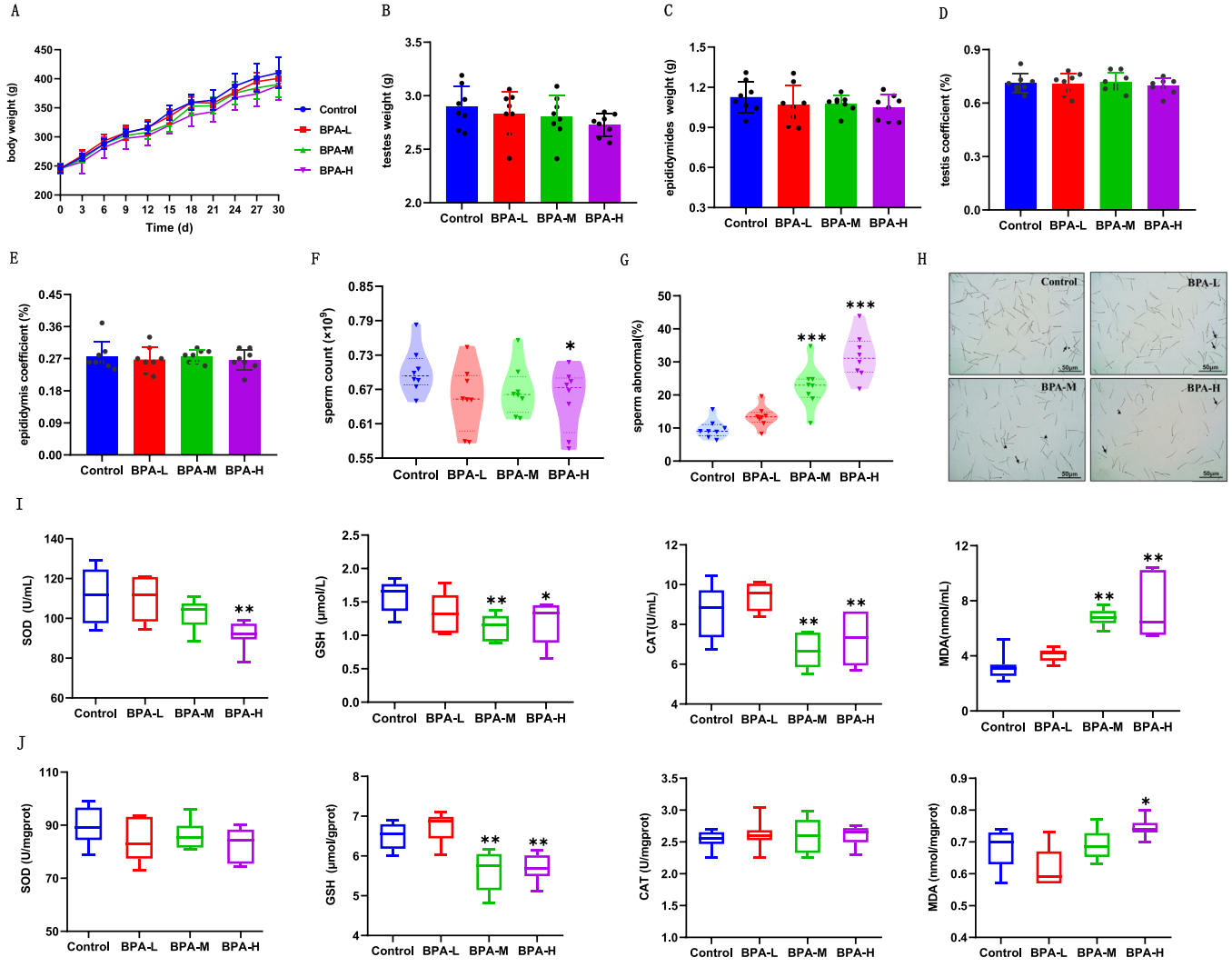

Fig. 1. Effects of BPA exposure on sperm quality, and oxidative stress in SD rats. (A) Body weight change. (B) Testis weight. (C) Epididymis weight. (D) Testis coefficient. (E) Epididymis coefficient. Sperm quality and morphology were analyzed by CASA. (F) Sperm counts. (G) Sperm abnormality. (H) Representative examples of sperm morphology. Abnormalities characterized by deformed or absent head (black arrows) and docked tail (black triangle) are seen in rats. (I) The levels of superoxide dismutase activity (SOD), glutathione (GSH), catalase activity (CAT), and malondialdehyde (MDA) in rat serum. (J) The levels of SOD, GSH, CAT, and MDA in rat testes. Data are expressed as mean ± SD (n = 8). Bars with different letters represent a significant difference between groups ($P < 0.05$).

analysis of variance (ANOVA), and the differences between the two groups were analyzed by the Bonferroni post hoc test. Values were considered to be significantly different when $P < 0.05$.

3. Results

3.1. Effects of BPA exposure on anthropomorphic parameters and sperm quality

Exposure to BPA led to a lower increase in the body weight of the rats over time when compared to the control animals (Fig. 1A). Body, testis, and epididymis weights and the coefficients of testes and epididymides were however not significantly affected by BPA treatment (Fig. 1B-E). Exposure to the high dose of BPA (BPA-H) notably decreased total sperm count compared with the controls ($P < 0.05$) (Fig. 1F, and H). Concomitantly, the sperm malformation ratio was significantly increased in the BPA-M, and BPA-H groups, characterized by the headless and tail-docking sperm ($P < 0.05$) (Fig. 1G).

3.2. Effects of BPA exposure on serum and testicular oxidative stress markers

To elucidate the presence of oxidative stress induced by BPA exposure, the levels of MDA and antioxidant markers SOD, GSH, and CAT were measured in rat serum and testis tissue homogenates. A significant decrease in serum SOD and CAT levels was observed in rats of the BPA-H group compared to the controls ($P < 0.05$) (Fig. 1I). GSH level was significantly decreased in the BPA-M group ($P < 0.05$) (Fig. 1I), while MDA content in serum and testis was higher in the BPA-M and BPA-H groups when compared to the control animals ($P < 0.05$) (Fig. 1I, J). As shown in Fig. 1J, exposure to BPA had no significant effects on the testicular levels of SOD and CAT, while a significant decrease in GSH level was observed in testis tissue in the BPA-M and BPA-H groups.

3.3. Effects of BPA exposure on testis and epididymis histology

As shown in Fig. 2A, the testis tissue showed a regular arrangement of different stages of germ cells in the seminiferous tubules of the control group in rats. Sertoli cells and spermatogonia were located on intact basement membranes. The slides from BPA-treated groups showed disorganization of the germinal epithelial layers of the seminiferous tubules. In the BPA-exposed groups, some seminiferous tubules showed mild atrophy as evidenced by the presence of vacuoles between the germ cells, while the interstitial space seemed enlarged. Maturation of sperm largely occurs in the epididymis; in the cauda epididymis, the sperm acquires motility. Fig. 2A gives the impression that sperm numbers are reduced in the BPA-M and BPA-H treated animals when compared to the controls, which is confirmed for the BPA-H group by the total sperm count shown in Fig. 1F.

3.4. Effects of BPA exposure on hormone levels

In this study, medium and high dosages of BPA administration significantly upregulated hypothalamic *Kiss1* mRNA expression ($P < 0.05$) (Fig. 2B). However, Fig. 2C revealed that there was a significant decrease in GPR54 mRNA expression in low and high groups. GnRH protein content in the hypothalamus was also significantly higher in the BPA-treated rats compared to the control group (Fig. 2D). Serum testosterone levels were reduced in the BPA-M and BPA-H groups compared to the untreated controls ($P < 0.05$) (Fig. 2E). Similarly, serum INHB level was significantly decreased in the BPA-H group ($P < 0.05$) (Fig. 2I), while FSH and DHT levels were significantly

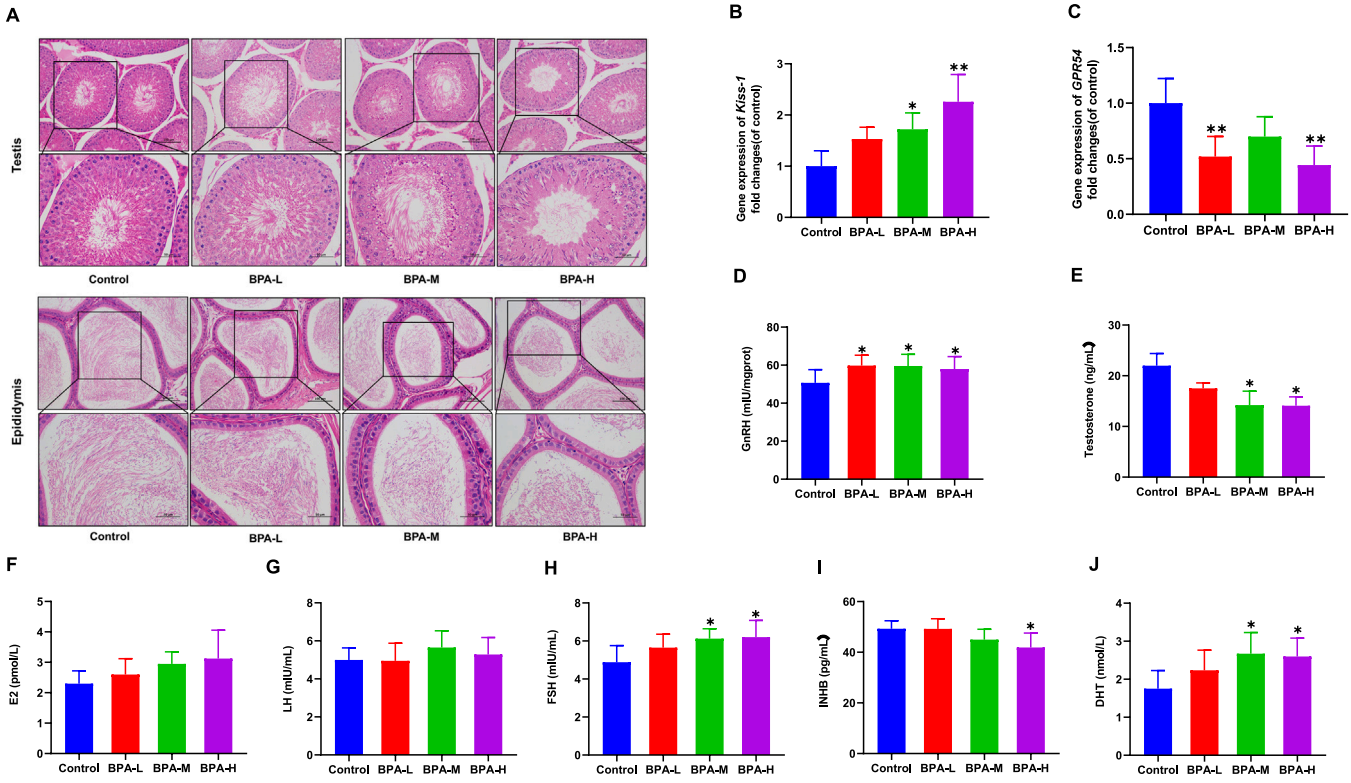

Fig. 2. Effects of BPA exposure on histology of testis and epididymis, and hormone levels. (A) Testis and epididymis. From left to right: control, BPA-L, BPA-M, BPA-H. Bar represents 50 μm and 100 μm, respectively. RT-PCR analyses of the mRNA levels of (B) *Kiss-1*, and (C) *Gpr54* in the hypothalamus. (D) GnRH protein content in the hypothalamus. The levels of (E) testosterone, (F) E2, (G) luteinizing hormone (LH), (H) follicle-stimulating hormone (FSH), (I) inhibin B (INHB), and (J) dihydrotestosterone (DHT) in rat serum was measured by ELISA. Data are expressed as mean ± SD (n = 8). Different letters represent a significant difference between groups ($P < 0.05$).

elevated in the BPA-M and BPA-H groups ($P < 0.05$) (Fig. 2H, J). There was no significant difference in E2 and LH levels among the different groups.

3.5. Effects of BPA exposure on PI3K/AKT/mTOR pathway in testis

To determine whether chronic BPA administration affects the PI3K/AKT/mTOR signaling pathway and in this way affects testis function, we investigated the relative expressions of key proteins and genes in this pathway by Western blotting and RT-PCR. As shown in Fig. 3A-C, exposure to BPA had no significant effect on the gene expression of *Pi3k*, *Akt,* and *mtor*. However, the protein levels of the PI3K in the high-dose group were significantly escalated in testis ($P < 0.05$) (Fig. 3D), as well as the level of p-AKT in medium and high dosage groups ($P < 0.05$) (Fig. 3F). Accordingly, the expression of PI3K and p-AKT determined by immunohistochemically staining were upregulated in BPA-treated groups. Moreover, we evaluated the localization of mTOR in the testis by immunohistochemistry. mTOR expression in rat testicular tissue was seen in Sertoli cells, spermatogonia, spermatocytes, and some Leydig cells. The protein level of mTOR was significantly increased in the testicular after being treated with medium and high dosage BPA compared with the control group (Fig. 3L). The protein expression of the Raptor was increased in the BPA-H group compared to the control group ($P < 0.01$) (Fig. 3I). Interestingly, the protein expression of 4EBP1 was significantly reduced in the BPA-M and BPA-H groups compared to the group ($P < 0.05$) (Fig. 3J), while the protein level of eIF4E was significantly increased (Fig. 3K).

3.6. Effects of BPA exposure on apoptosis in testes

Apoptosis is one of the main forms of cell death in which mitochondria play a key role. To explore whether chronic BPA exposure leads to an increase in testicular apoptosis, we examined the expression of apoptosis-related proteins by western blot. As illustrated in Fig. 4A-G, a significant increase was observed in cleaved-PARP/PARP, FAS, and Caspase3 levels after exposure to the high dosage of BPA. No significant difference was observed in the levels of FASL, Bax, and Bcl-2 compared to the control group ($P < 0.05$) (Fig. 4C, F, and G). In addition, apoptotic cells in the testes section were subsequently detected by TUNEL staining. As shown in Fig. 4H, BPA-induced apoptosis occurs in both Leydig cells and germ cells which is characterized by spermatogonia and spermatocytes compared to the control. These results indicated that BPA treatment may increase the incidence of apoptosis to some extent.

3.7. Effects of BPA exposure on histone ubiquitination in testes

To comprehend the expression of H2A, H2B, ub-H2A, ub-H2B, H3, and H4 in the testes, western blotting was applied to observe the expressions of these parameters in rats from different groups. H2A and H3 expressions were higher in the medium and high groups ($P < 0.05$, $P < 0.01$) (Fig. 5A, B, and F), while ubiquitin histone H2A (ub-H2A) and ubiquitin histone H2B (ub-H2B) was markedly reduced in BPA-exposure groups compared with the control group (Fig. 5A, D, and E). There was no significance in the H2B and H4 protein expressions (Fig. 5C, G).

3.8. Effects of BPA exposure on gut microbiota composition

To determine whether BPA treatment affects gut microbiota composition, we analyzed the 16S rRNA gene sequence of the microbiota. Generally, α-diversity reflects the abundance of the gut microbiota, and β-diversity is used to evaluate the community similarity and diversity of different groups. As shown in Fig. 6A, the PCA reflecting the β-diversity showed an obvious separation among the groups, which means that the intestinal microbiota composition changed significantly after treatment with BPA. The BPA-M and BPA-H groups exhibited significantly lower Chao1 and higher goods coverage ($P < 0.05$, $P < 0.01$) (Fig. 6B, C). Shannon (Fig. 6D) showed a downward trend in medium and high groups, implying that BPA exposure may lead to lower intestinal microbiota diversity. The composition of gut microbiota among the groups at the phylum, class, order, and family levels is shown in Fig. 6E-H. At the phylum level, the main gut microbiota were *Bacteroidetes* (66.21% vs 73.96% vs 71.71% vs 63.3%), *Firmicutes* (26.23% vs 22.65% vs 23.26% vs 29.06%), *Proteobacteria* (2.48% vs 2.26% vs2.63% vs 4.90%), and *Epsilonbacteraeota* (4.47% vs 0.5% vs 1.71% vs 1.85%) in Control, BPA-L, M, and H groups, respectively. The relative abundance of class *Campylobacteria* were 4.45%, 0.6%, 1.69%, and 1.80%, whereas *Gammaproteobacteria* were 0.83%, 1.23%, 1.81%, and 3.97% in Control, BPA-L, M, and H groups, respectively (Fig. 6F). At the order level, the BPA-L group showed a lower abundance of *Campylobacterales* (0.48%) compared to the control rats (4.37%). In addition, the relative abundance of *Betaproteobacteriales* was increased in the BPA-H group (2.32%) compared to the control rats (0.63%) (Fig. 6G). However, there was no significant difference in the main microbiota at the family level among groups.

3.9. Correlations between the intestinal microbiota and hormone parameters

To confirm the significant differences in microbiota composition and identify biomarkers in intestinal microbiota among the treatment groups, we applied LEfSe, an algorithm for microbial marker detection. As depicted in Fig. 7A and B, the differential enrichment of specific bacteria was shown in both cladograms and histograms based on an LDA score > 3. For the control group, the genus *Prevotellaceae_Ga6A1_group*, and genus *Lachnospiraceae_NK4A136_group* were the dominant microbiota, while the genus *Alloprevotella*, genus *uncultured_organism*, and genus *Prevotellaceae_UCG_001* appeared to be dominant in the BPA-M group. The LEfSe histogram showed further that the BPA-H group contained the largest number of bacterial taxa, suggesting that the BPA effect on the bacterial community composition mainly depended on the doses. Furthermore, we observed that the relative abundance of the class *Gammaproteobacteria* and the genus *Parasutterella*, family *Burkholderiaceae*, order *Enterobacteriales* were significantly higher in the BPA-H group than in the control group, suggesting that these may serve as taxonomic biomarkers.

The correlation analysis with a heatmap indicated that the relative abundance of several key intestinal microbial phylotypes was significantly correlated with the reproductive hormones.

Parameters (Fig. 7C). *Fusicatenibacter* was notably positively correlated with serum DHT, E2 levels, and *kiss-1* expression in the hypothalamus, while a negative correlation was observed with testosterone levels. *Desulfovibrio*, *Ruminiclostridium*, *Acetatifactor*, *Rikenella*, *and Ruminiclostridium_5* were negatively correlated with serum FSH, LH, DHT, and E2 levels, and *kiss-1* expression in the hypothalamus, and positively correlated with serum INHB and testosterone levels, GnRH protein level and *Gpr54* gene expression in the hypothalamus. Overall, most of the bacterial genera of composition were altered by BPA administration and exhibited strong correlations with hormones.

4. Discussion

Reports have demonstrated that BPA is a part of many aspects of daily living, as a variety of common consumer goods ranging from water bottles, dinner plates, and CDs (Wang et al., 2014). BPA can disrupt the endocrine function related to hormone levels due to its estrogenic and antiandrogenic activity and is known to affect male fertility (Cariati et al., 2019). Although the effect of BPA on the testis has been studied, whether BPA-induced male reproductive toxicity is associated with the alteration of gut microbiota has remained largely unknown. In the present study, in vivo experiment with multiple dimensions analysis was conducted to elucidate the potential mechanism of BPA exposure on the reproductive system in male rats.

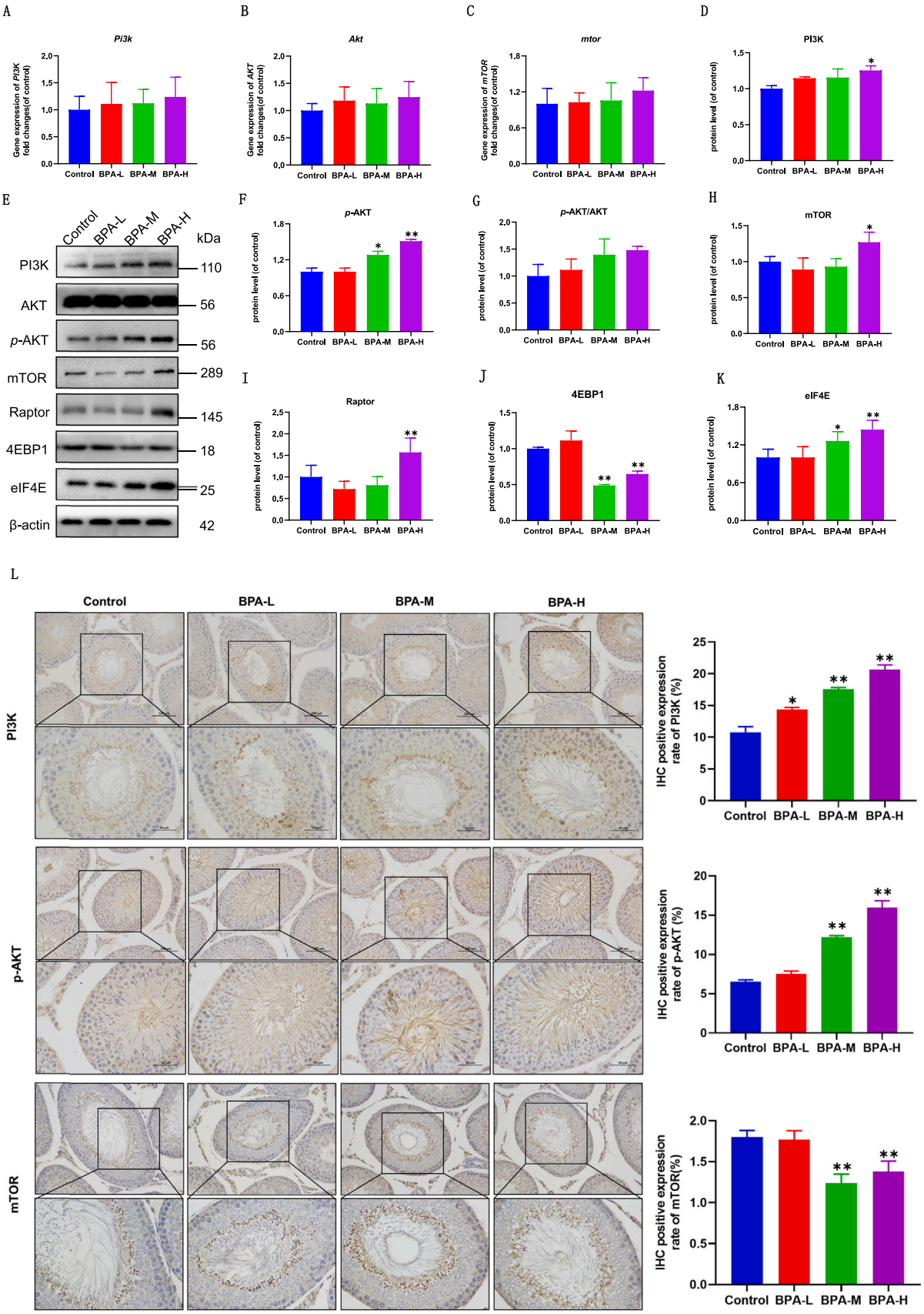

Fig. 3. Effects of BPA exposure on PI3K/AKT/mTOR pathway in testis (A-C) The mRNA expression levels of *Pi3k*, *Akt1*, and *mtor* in testis. (D-K) The protein expression levels of PI3K, mTOR, p-AKT, p-AKT/AKT, Raptor, 4EBP1, and eIF4E in testis. Different letters indicate significant differences between groups ($P < 0.05$). (L) Immunohistochemical staining for PI3K, p-AKT, and mTOR proteins in testes tissue (200×, 400× magnifications). Quantitative data are presented as mean ± SD (n = 4). * $P < 0.05$, ** $P < 0.01$, compared with control group.

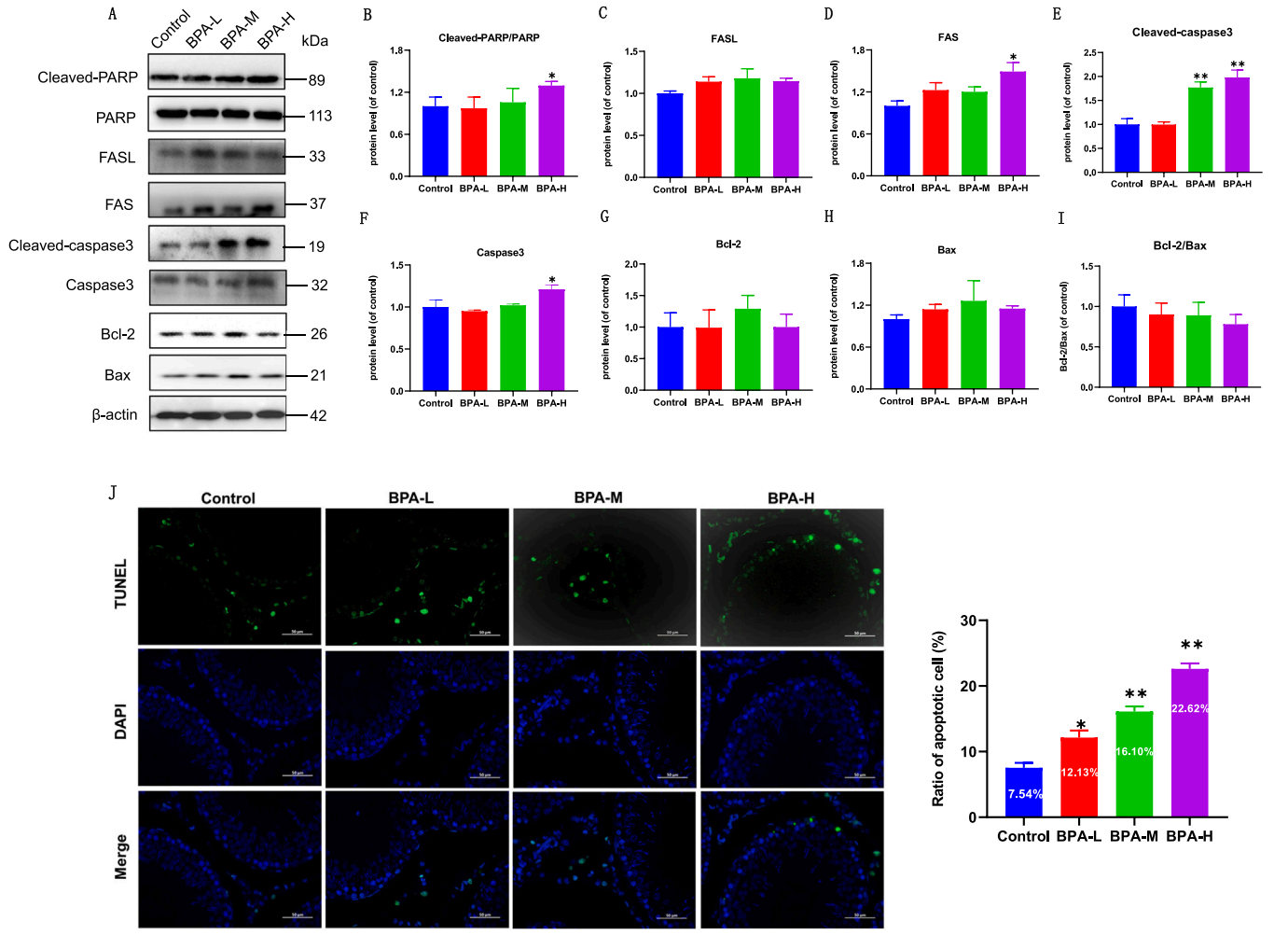

Fig. 4. Effects of BPA exposure on cell apoptosis in testes. (A) Western blotting photographs and relative quantitative analysis of (B) Cleaved-PARP and PARP protein, (C) FASL, (D) FAS, (E) Cleaved-caspase3, (F) Caspase3, (G) Bcl-2, (H) Bax, and (I) Bcl-2/Bax. Data are expressed as mean ± SD (n = 4). Different letters indicate significant differences between groups ($P < 0.05$). (H) The assessment of apoptosis in testes sections with TUNEL immunofluorescence and the ratio of apoptosis cells were counted in every field. Quantitative data are presented as mean ± SD (n = 4). * $P < 0.05$, ** $P < 0.01$, compared with control group.

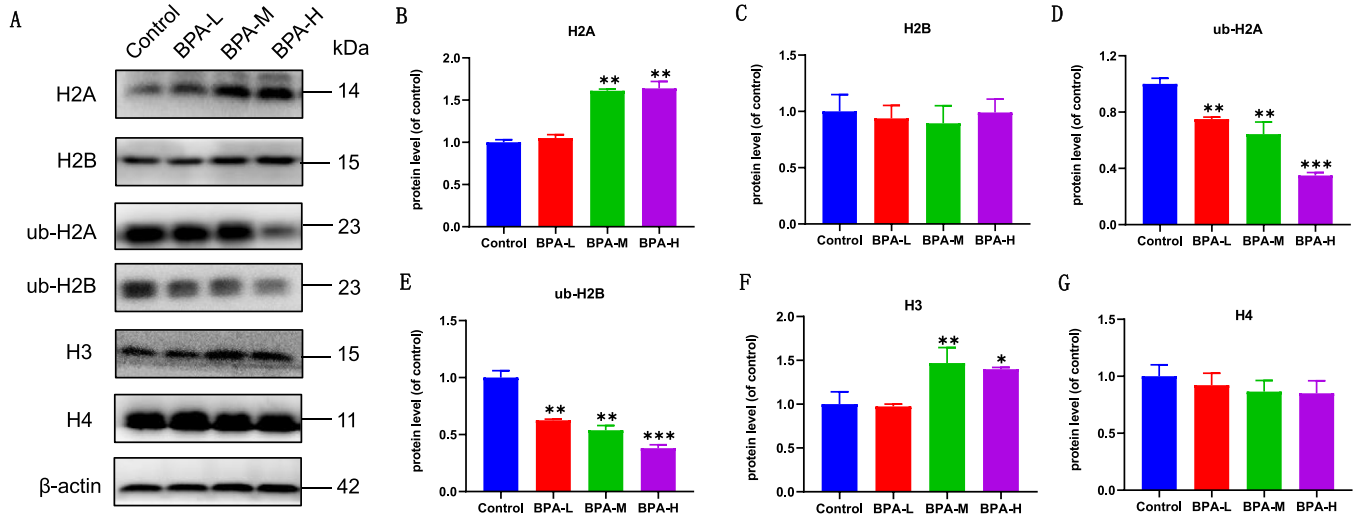

Fig. 5. Effects of BPA exposure on the levels of histone ubiquitination in testes. (A) Representative western blots and relative quantitative analysis of (B) H2A, (C) H2B, (D) ub-H2A, (E) ub-H2B, (F) H3, and (G) H4. The data are expressed as mean ± SD (n = 4). Different letters indicate significant differences between groups ($P < 0.05$).

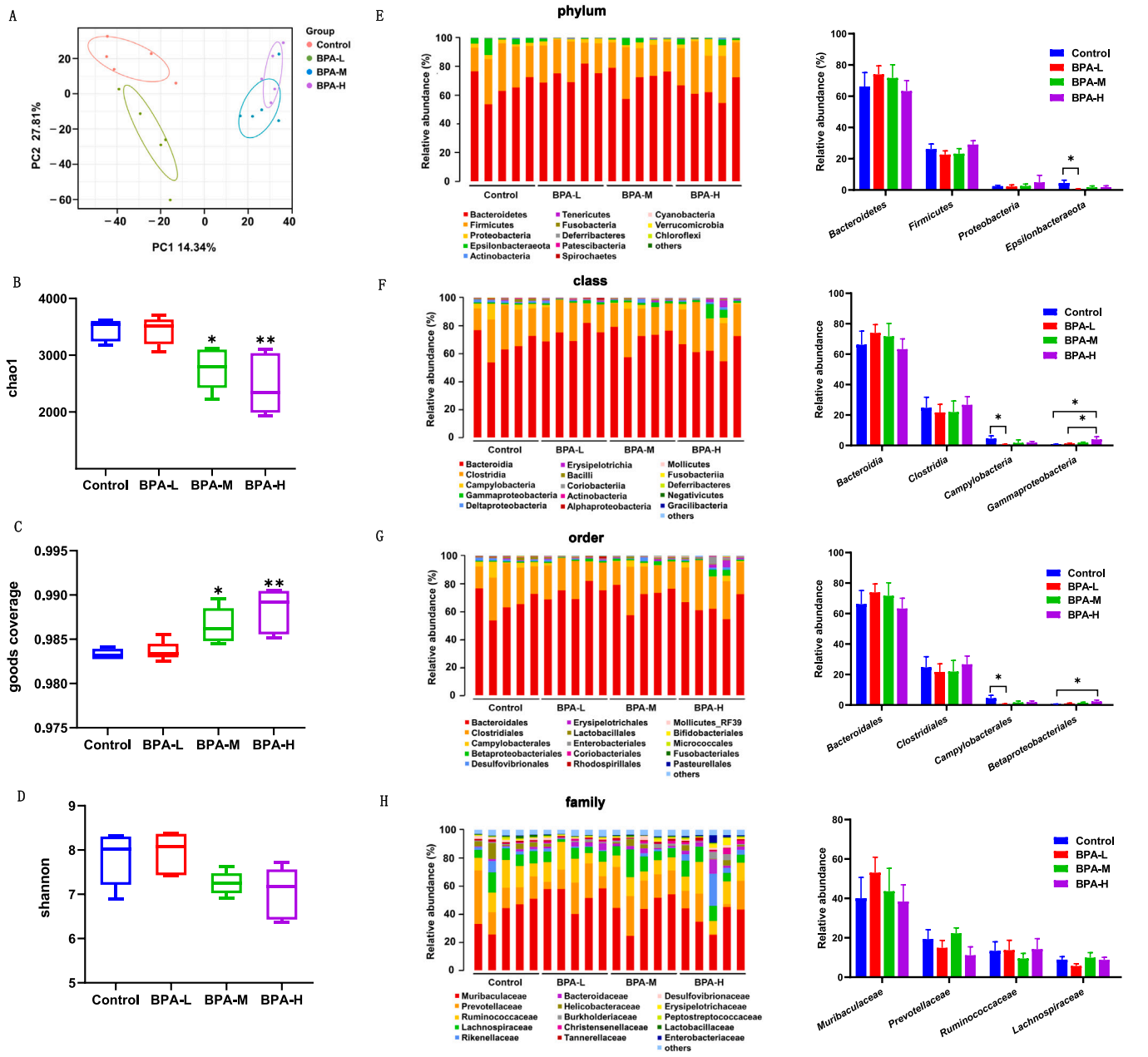

Fig. 6. Effects of BPA exposure on gut microbiota composition of rats. (A) Principal component analysis (PCA) of gut bacterial community composition. α-diversity analysis: (B) Chao1 index, (C) Shannon index, and (D) Simpson index. Composition of microbial community and the main microbiota at (E) phylum, (F) class, (G) order, and (H) family level. Statistical significance was determined by one-way ANOVA and the LSD post-hoc test, * $P < 0.05$, ** $P < 0.01$ compared to the control group.

Spermatogenesis is a highly ordered and precisely regulated process, which requires huge epigenetic remodeling (Govin et al., 2006). Normal spermatogenesis is dependent on well-balanced spermatogenetic cell proliferation, differentiation, and death in the testes (Zhang et al., 2012). LH stimulated the production of testosterone by Leydig cells, and FSH stimulated the local production of estradiol by Sertoli cells. Besides, FSH and testosterone directly control the expression of genes in Sertoli cells which are required for the progression of meiotic and post-meiotic events (O'Shaughnessy et al., 2010). Normal testosterone levels are necessary for maintaining the development of the male reproductive system (Zhao et al., 2020). In our study, a high dose of BPA-treated rats showed less sperm count while a higher deformity rate significantly. And the decreased levels of testosterone further confirmed the disruption of hormones involved in the BPA-induced testicular toxicity. The testicular normal structure is important for maintaining normal reproductive function. And the histopathological examination of testis and epididymis is also important for fertility diagnosis and prognosis inference in reproductive practice (McLachlan et al., 2007). Consistent with the data on sperm quality, we observed disarrangement of testicular tissue, and atrophy of spermatogenic tubules in a dose-dependent manner, suggesting that BPA influences spermatogenesis.

The kisspeptin system is a key regulator of the reproductive system, and the formation and function of the kisspeptin signaling pathway are affected by sex hormones at different stages of the life cycle, which can regulate the reproductive endocrine system. *Kiss-1* gene, as a target for regulation by testosterone, the increased expression of GnRH, and FSH can also be understood as negative feedback regulation of testosterone. The upregulation of hypothalamic Kiss-1 after BPA exposure may stimulate the synthesis and release of GnRH and gonadotropins in the hypothalamus and pituitary gland, respectively (Xi et al., 2011). In the

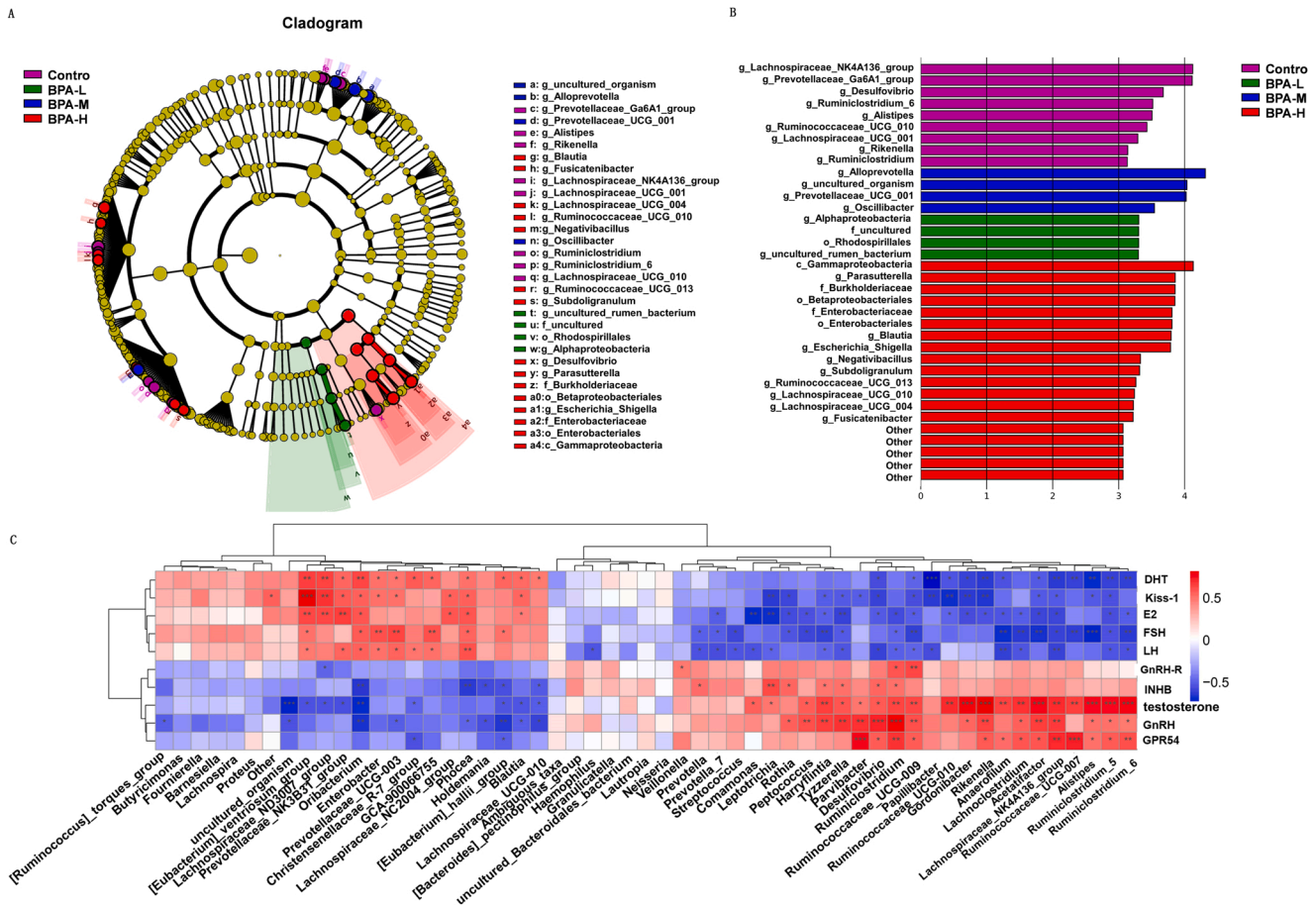

Fig. 7. Correlations between the intestinal microbiota and hormone parameters. (A) Cladograms based on LEfSe analysis representing featuring bacterial taxa. (B) LDA score, each taxon with a threshold score larger than 3 is shown in the histogram, the bar length of LDA represents the impact of significantly different species in each group. (C) Correlation analysis between intestinal flora and hormones in rats. Spearman's correlation coefficients are represented by color ranging from blue, negative correlation (−0.5), to red, positive correlation (0.5). Significant correlations are noted by * $P < 0.05$, ** $P < 0.01$, and *** $P < 0.001$.

present study, we observed that BPA exposure decreased INHB levels in serum, and increased the FSH and DHT levels. The decrease in INHB may be indicative of a BPA-induced alteration of Sertoli cell functionality. The effects on seminiferous epithelium morphology are relatively mild which may be due to a compensatory effect by DHT, a metabolite of testosterone that binds with a substantially higher affinity to the androgen receptor than testosterone (Carson and Rittmaster, 2003). Moreover, in line with the increased *Kiss-1* expression in the hypothalamic, *GnRH* gene expression in the pituitary increased, which is similar to a study by Oride et al. who showed that clomiphene citrate induced *Kiss-1* expression in the presence of estradiol in mHypoA-50 cells (Oride et al., 2020). These results suggest that BPA exposure disrupted the imbalance of hormones, further leading to a suboptimal maturation of the spermatids and being responsible for the observed increased sperm malformation.

As another concerned item, the process of spermatogenesis was regulated by histone modification accurately, and the histone ubiquitination process is the master prerequisite of nucleosome removal during the sperm elongating period (Zhao et al., 2022). As the first step in histone-to-protamine exchange, histone ubiquitination can promote histone removal by loosening the compact nucleosome, subsequently, promoting the replacement of transition protein in pachytene spermatocyte (Li et al., 2020). In our study, the protein expression of H2A and H3 were significantly increased in medium and high doses of BPA-treated groups, while the ubiquitinated histone H2A and ubiquitinated H2B were significantly diminished. Therefore, these data indicated BPA exposure affected spermatogenesis by altering the ubiquitination.

Testicular cells contain a large amount of unsaturated fatty acids and divide at a high speed, which makes spermatogenic cells highly susceptible to oxidative damage, which is not conducive to sperm production (Sharma et al., 2019). Reactive oxygen species (ROS) are involved in DNA damage, resulting in the status of oxidative stress and possibly modulating the apoptotic pathway. SOD can catalyze the overproduced O_2^- into H_2O_2, next H_2O_2 is catalyzed into H_2O and O_2 by CAT, which protected the body from harmful substances-induced oxidative stress. GSH is a crucial non-protein antioxidant and can scavenge the lipid peroxide radicals. When an exogenous substance enters the body, it will be slowly released into the blood, and then reach organs through the blood. Therefore, the oxidation indicators in the blood are the first to be observed when the body is oxidized and injured. That is the reason that the SOD and CAT activities were significantly increased in the blood compared to the control group in this study. While the lipid peroxidative products exceed the scavenging efficiency of GSH, it will accumulate in the blood and tissues, and there is a significant increase in GSH. Histones can migrate from the nucleus into the cytoplasm as a response to DNA double-strand breakage and then can indirectly activate BAK at the mitochondrial outer membrane, resulting in the promotion of cytochrome C release and activation of a cell programmed apoptosis. In our study, we found that the protein levels of Cleaved-PARP/PARP and FAS were significantly increased in the BPA-H group, as well as the percentage of TUNEL-positive cells in rat testes expoto sed BPA. Cleaved-caspase3, which is the main final executor of apoptosis, is responsible for the cleavage of key cellular proteins, leading

to apoptosis (Budihardjoetal.,1999). Increased activities of Cleaved-caspase3 in this study proved that caspase cascades are involved in BPA-induced spermatogenic cell apoptosis. However, there was no significant change in Bcl-2 and Bax. We speculated that the apoptosis of testis tissue induced by BPA may be mainly affecting the FAS pathway rather than the Bax pathway.

The process of germ cell development is under the tight control of various signaling pathways, including the PI3K/Akt/mTOR pathway. A previous study has confirmed that PI3K/AKT/mTOR signaling pathway is one of the classical pathways to inhibit apoptosis (Wu et al., 2020). Moreover, FSH can regulate Sertoli cell proliferation through the pathway (Riera et al., 2012). The germ cells in the testis are highly proliferative and metabolically active. It is therefore not surprising that the PI3K/AKT/mTOR pathway plays a central role in the self-renewal of spermatogonial stem cells and the proliferation and differentiation of spermatogonia (Moreira et al., 2019; Cao et al., 2020; Zhang et al., 2020). Therefore, we next evaluated the PI3K/AKT pathway. The current data show that BPA exposure leads to activation of the PI3K/AKT pathway in testes of male SD rats. Meanwhile, the inhibition of mTOR may interfere with Sertoli cell functionality, leading to the premature release of sperm cells (Boyer et al., 2016). Therefore, we speculate it is probably a protective compensation reaction, that is the activation of AKT can protect cells from damage under oxidative stress.

Gut microbiota plays a role in metabolic disorders and participates in the regulation of hormonal levels, estrous cycle, and reproductive functions (Hussain et al., 2021). A previous study showed that gut microbes can involve in estrogen and androgen cycling and influence sex steroid hormone levels, as well as androgen production from glucocorticoids (Cross et al., 2018). Sexual maturation was a major determinant of the cecal microbiome community structure, and microbial colonization status was correlated with testosterone levels. The removal of the gut microbiota decreases testosterone levels in male mice, indicative of bidirectional interaction between the amount of male sex hormone and the microbiota (Markle et al., 2013). In addition, a previous study indicated that testosterone may be one of the indirect factors leading to the development of amphoteric colon adenoma (Amos-Landgraf et al., 2014). In turn, the gut microbiota itself also influences estrogen levels (Rizzetto et al., 2018). The present study showed that BPA exposure caused gut microbial dysbiosis, with lower diversity in α-diversity and altered relative abundance for certain bacterial taxa. *Bacteroidetes,* and *Firmicutes*, which accounted for up to 90% of the total sequences, were the dominant phylum in BPA-treated groups. The relative abundances of the class *Gammaproteobacteria* and the order *Betaproteobacteriales* were elevated after exposure to the high dose of BPA. Ni et al. (2021) have found that BPA exposure increases the abundance of *Firmicutes* and decreases the abundance of *Bacteroidetes* in C57BL/6 male mice. *Proteus* is anaerobic or facultative anaerobic bacillus in the gastrointestinal tract and hydrolyzes urea into ammonia and carbon dioxide via urease (Fan et al., 2020). *Gammaproteobacteria* are involved in the synthesis of vitamin B12 and have multiple beneficial functions in the intestine including the synthesis and uptake of amino acids (Paris et al., 2020). Therefore, we speculate that BPA may increase the permeability of the intestinal barrier by altering the gut microbiome. This pathological change may induce the likelihood that bacterial pathogens will enter the systemic circulation, which may affect the secretion of hormones in the body (Ait-Belgnaoui et al., 2012).

In future research, the contents of different bacteria and multi-omic techniques such as proteomics, and metabolomics are needed to reveal novel interactions between gut microbiota and sex hormones.

5. Conclusion

In summary, BPA-induced gut microflora disorder is closely related to male reproductive toxicity. Disorder of sex hormone levels is strongly associated with the imbalance of intestinal flora. BPA exposure affected spermatogenesis by increasing oxidative stress and leading to mitochondria apoptosis. In addition, the histone modification was perturbed, and the PI3K/AKT pathway was activated in rat testicular after exposure to BPA. Further research is needed to investigate the mechanisms of those identified key microbiota as a biomarker for certain reproduction-related diseases.

Funding

This work was supported by the Youth Science and Technology Innovation Talent of Guangdong TeZhi Plan (No. 2019TQ05N770); Guangdong Basic and Applied Basic Research Foundation (No. 2020A1515111045); Guangdong Key Area Research and Development Program (No. 2019B020210003); Construction Plan of Guangdong Province High-level Universities and the Research Start-up Funds for the High-level Talent Introduction Project of South China Agricultural University (No. 20173326).

CRediT authorship contribution statement

Ruijing Liu: Investigation, Formal analysis, Methodology, Writing – original draft. **Dongbao Cai:** Methodology, Data curation. **Xusheng Li:** Data curation, Validation. Writing – review & editing. **Boping Liu:** Funding acquisition, Project administration, Writing – review & editing. **Jiali Chen:** Methodology. **Xinwei Jiang:** Methodology. **Haiwei Li:** Methodology, Visualization. **Zhenhua Li:** Methodology. **Katja Teerds:** Writing – review & editing. **Jianxia Sun:** Data curation. **Weibin Bai:** Conceptualization, Funding acquisition, Project administration, Resources, Supervision. **Yulong Jin:** Data curation, Funding acquisition, Writing – review & editing, Supervision.

Declaration of Competing Interest

The authors declare that they have no known competing financial interests or personal relationships that could have appeared to influence the work reported in this paper.

References

Adegoke, E.O., Rahman, M.S., Amjad, S., Pang, W.K., Ryu, D.Y., Park, Y.J., Pang, M.G., 2022. Bisphenol A damages testicular junctional proteins transgenerationally in mice. Environ. Pollut. 302, 119067 https://doi.org/10.1016/j.envpol.2022.119067.

Ait-Belgnaoui, A., Durand, H., Cartier, C., Chaumaz, G., Eutamene, H., Ferrier, L., Houdeau, E., Fioramonti, J., Bueno, L., Theodorou, V., 2012. Prevention of gut leakiness by a probiotic treatment leads to attenuated HPA response to an acute psychological stress in rats. Psychoneuroendocrinology 37, 1885–1895. https://doi.org/10.1016/j.psyneuen.2012.03.024.

Amos-Landgraf, J.M., Heijmans, J., Wielenga, M.C., Dunkin, E., Krentz, K.J., Clipson, L., Ederveen, A.G., Groothuis, P.G., Mosselman, S., Muncan, V., Hommes, D.W., Shedlovsky, A., Dove, W.F., van den Brink, G.R., 2014. Sex disparity in colonic adenomagenesis involves promotion by male hormones, not protection by female hormones. Proc. Natl. Acad. Sci. USA 111, 16514–16519. https://doi.org/10.1073/pnas.1323064111.

Boyer, A., Girard, M., Thimmanahalli, D.S., Levasseur, A., Céleste, C., Paquet, M., Duggavathi, R., Boerboom, D., 2016. mTOR regulates gap junction Alpha-1 protein trafficking in sertoli cells and is required for the maintenance of spermatogenesis in mice. Biol. Reprod. 95, 13. https://doi.org/10.1095/biolreprod.115.138016.

Buckley, J.P., Kim, H., Wong, E., Rebholz, C.M., 2019. Ultra-processed food consumption and exposure to phthalates and bisphenols in the US National Health and Nutrition Examination Survey, 2013-2014. Environ. Int. 131, 105057 https://doi.org/10.1016/j.envint.2019.105057.

Calafat, A.M., Ye, X., Wong, L., Reidy, J.A., Needham, L.L., 2008. Exposure of the U.S. population to bisphenol A and 4-tertiary-octylphenol: 2003-2004. Environ. Health Perspect. 116, 39–44. https://doi.org/10.1289/ehp.10753.

Cao, J., Lin, Z., Tong, M., Zhang, Y., Li, Y., Zhou, Y., 2020. Mechanistic target of rapamycin kinase (Mtor) is required for spermatogonial proliferation and differentiation in mice. Asian J. Androl. 22, 169–176. https://doi.org/10.4103/aja.aja_14_19.

Cariati, F., D'Uonno, N., Borrillo, F., Iervolino, S., Galdiero, G., Tomaiuolo, R., 2019. Bisphenol a: an emerging threat to male fertility. Reprod. Biol. Endocrinol. 17, 6. https://doi.org/10.1186/s12958-018-0447-6.

Carson, C., Rittmaster, R., 2003. The role of dihydrotestosterone in benign prostatic hyperplasia. Urology 61, 2–7. https://doi.org/10.1016/s0090-4295(03)00045-1.

Cho, S., Choi, Y.S., Luu, H.M., Guo, J., 2012. Determination of total leachable bisphenol A from polysulfone membranes based on multiple consecutive extractions. Talanta 101, 537–540. https://doi.org/10.1016/j.talanta.2012.09.033.
Corradi, P.F., Corradi, R.B., Greene, L.W., 2016. Physiology of the hypothalamic pituitary gonadal axis in the male. Urol. Clin. N. Am. 43, 151–162. https://doi.org/10.1016/j.ucl.2016.01.001.
Cross, T.L., Kasahara, K., Rey, F.E., 2018. Sexual dimorphism of cardiometabolic dysfunction: gut microbiome in the play? Mol. Metab. 15, 70–81.
Demierre, A., Peter, R., Oberli, A., Bourqui-Pittet, M., 2012. Dermal penetration of bisphenol A in human skin contributes marginally to total exposure. Toxicol. Lett. 213, 305–308. https://doi.org/10.1016/j.toxlet.2012.07.001.
Diamante, G., Cely, I., Zamora, Z., Ding, J., Blencowe, M., Lang, J., Bline, A., Singh, M., Lusis, A.J., Yang, X., 2021. Systems toxicogenomics of prenatal low-dose BPA exposure on liver metabolic pathways, gut microbiota, and metabolic health in mice. Environ. Int. 146, 106260 https://doi.org/10.1016/j.envint.2020.106260.
Ehrlich, S., Calafat, A.M., Humblet, O., Smith, T., Hauser, R., 2014. Handling of thermal receipts as a source of exposure to bisphenol A. JAMA 311, 859–860. https://doi.org/10.1001/jama.2013.283735.
Fan, S., Li, H., Zhao, R., 2020. Effects of normoxic and hypoxic conditions on the immune response and gut microbiota of Bostrichthys sinensis. Aquaculture 525, 735336. https://doi.org/10.1016/j.aquaculture.2020.735336.
Fu, G., Dai, J., Li, Z., Chen, F., Liu, L., Yi, L., Teng, Z., Quan, C., Zhang, L., Zhou, T., Donkersley, P., Song, S., Shi, Y., 2020. The role of STAT3/p53 and PI3K-Akt-mTOR signaling pathway on DEHP-induced reproductive toxicity in pubertal male rat. Toxicol. Appl. Pharmacol. 404, 115151 https://doi.org/10.1016/j.taap.2020.115151.
Gao, L., Dong, Y., Lin, R., Meng, Y., Wu, F., Jia, L., 2020. The imbalance of Treg/Th17 cells induced by perinatal bisphenol A exposure is associated with activation of the PI3K/Akt/mTOR signaling pathway in male offspring mice. Food Chem. Toxicol. 137, 111177 https://doi.org/10.1016/j.fct.2020.111177.
Gou, L., Kang, J., Dai, P., Wang, X., Li, F., Zhao, S., Zhang, M., Hua, M., Lu, Y., Zhu, Y., Li, Z., Chen, H., Wu, L., Li, D., Fu, X., Li, J., Shi, H., Liu, M., 2017. Ubiquitination-deficient mutations in human piwi cause male infertility by impairing histone-to protamine exchange during spermiogenesis. Cell 169, 1090–1104. https://doi.org/10.1016/j.cell.2017.04.034.
Govin, J., Lestrat, C., Caron, C., Pivot-Pajot, C., Rousseaux, S., Khochbin, S., 2006. Histone acetylation-mediated chromatin compaction during mouse spermatogenesis. Ernst Schering Res. Found. Workshop 57, 155–172. https://doi.org/10.1007/3-540-37633-x_9.
Health Canada, 2015. Third Report on Human Biomonitoring of Environmental Chemicals in Canada: Results of the Canadian Health Measures Survey Cycle 3 (2012–2013). Available online: ⟨https://www.canada.ca/en/health-canada/services/environmental-workplace-health/reports-publications/environmental-contaminants/third-report-human-biomonitoring-environmental-chemicals-canada.html⟩.
Hu, J., Raikhel, V., Gopalakrishnan, K., Fernandez-Hernandez, H., Lambertini, L., Manservisi, F., Falcioni, L., Bua, L., Belpoggi, F., L. Teitelbaum, S., Chen, J., 2016. Effect of postnatal low-dose exposure to environmental chemicals on the gut microbiome in a rodent model. Microbiome 4, 26. https://doi.org/10.1186/s40168-016-0173-2.
Hussain, T., Murtaza, G., Kalhoro, D.H., Kalhoro, M.S., Metwally, E., Chughtai, M.I., Mazhar, M.U., Khan, S.A., 2021. Relationship between gut microbiota and host-metabolism: emphasis on hormones related to reproductive function. Anim. Nutr. 7, 1–10. https://doi.org/10.1016/j.aninu.2020.11.005.
Javurek, A.B., Spollen, W.G., Johnson, S.A., Bivens, N.J., Bromert, K.H., Givan, S.A., Rosenfeld, C.S., 2016. Effects of exposure to bisphenol A and ethinyl estradiol on the gut microbiota of parents and their offspring in a rodent model. Gut Microbes 7, 471–485. https://doi.org/10.1080/19490976.2016.1234657.
Jiang, X., Zhu, C., Li, X., Sun, J., Tian, L., Bai, W., 2018. Cyanidin-3-O-glucoside at low doses protected against 3-Chloro-1,2-propanediol induced testis injury and improved spermatogenesis in male rats. J. Agric. Food Chem. 66, 12675–12684. https://doi.org/10.1021/acs.jafc.8b04229.
Kong, L., Wu, Y., Hu, W., Liu, L., Xue, Y., Liang, G., 2021. Mechanisms underlying reproductive toxicity induced by nickel nanoparticles identified by comprehensive gene expression analysis in GC-1 spg cells. Environ. Pollut. 275, 116556 https://doi.org/10.1016/j.envpol.2021.116556.
Lai, K., Chung, Y., Li, R., Wan, H., Wong, C.K., 2016. Bisphenol A alters gut microbiome: comparative metagenomics analysis. Environ. Pollut. 218, 923–930. https://doi.org/10.1016/j.envpol.2016.08.039.
Li, X., Yao, Z., Yang, D., Jiang, X., Sun, J., Tian, L., Hu, J., Wu, B., Bai, W., 2020. Cyanidin-3-O-glucoside restores spermatogenic dysfunction in cadmium-exposed pubertal mice via histone ubiquitination and mitigating oxidative damage. J. Hazard. Mater. 387, 121706 https://doi.org/10.1016/j.jhazmat.2019.121706.
Liu, J., Li, X., Zhou, G., Zhang, Y., Sang, Y., Wang, J., Li, Y., Ge, W., Sun, Z., Zhou, X., 2021a. Silica nanoparticles inhibiting the differentiation of round spermatid and chromatin remodeling of haploid period via MIWI in mice. Environ. Pollut. 284, 117446 https://doi.org/10.1016/j.envpol.2021.117446.
Liu, X., Wang, Z., Liu, F., 2021b. Chronic exposure of BPA impairs male germ cell proliferation and induces lower sperm quality in male mice. Chemosphere 262, 127880. https://doi.org/10.1016/j.chemosphere.2020.127880.
Markle, J.G.M., Frank, D.N., Mortin-Toth, S., Robertson, C.E., Feazel, L.M., Rolle-Kampczyk, U., von Bergen, M., McCoy, K.D., Macpherson, A.J., Danska, J.S., 2013. Sex differences in the gut microbiome drive hormone-dependent regulation of autoimmunity. Science 339, 1084–1088. https://doi.org/10.1126/science.1233521.
McLachlan, R.I., Rajpert-De, M.E., Hoei-Hansen, C.E., de Kretser, D.M., Skakkebaek, N.E., 2007. Histological evaluation of the human testis–approaches to optimizing the clinical value of the assessment: mini review. Hum. Reprod. 22, 2–16. https://doi.org/10.1093/humrep/del279.
Molina, A., Abril, N., Morales-Prieto, N., Monterde, J., Ayala, N., Lora, A., Moyano, R., 2018. Hypothalamic-pituitary-ovarian axis perturbation in the basis of bisphenol A (BPA) reproductive toxicity in female zebrafish (Danio rerio). Ecotoxicol. Environ. Saf. 156, 116–124. https://doi.org/10.1016/j.ecoenv.2018.03.029.
Moreira, B.P., Oliveira, P.F., Alves, M.G., 2019. Molecular mechanisms controlled by mTOR in male reproductive system. Int. J. Mol. Sci. 20, 1633. https://doi.org/10.3390/ijms20071633.
Murata, M., Kang, J., 2018. Bisphenol A (BPA) and cell signaling pathways. Biotechnol. Adv. 36, 311–327. https://doi.org/10.1016/j.biotechadv.2017.12.002.
Ni, Z., Sun, W., Li, R., Yang, M., Zhang, F., Chang, X., Li, W., Zhou, Z., 2021. Fluorochloridone induces autophagy in TM4 Sertoli cells: involvement of ROS-mediated AKT-mTOR signaling pathway. Reprod. Biol. Endocrinol. 19, 64. https://doi.org/10.1186/s12958-021-00739-8.
Oride, A., Kanasaki, H., Tumurbaatar, T., Zolzaya, T., Okada, H., Hara, T., Kyo, S., 2020. Effects of the fertility drugs clomiphene citrate and letrozole on kiss-1 expression in hypothalamic kiss-1 expressing cell models. Reprod. Sci. 27, 806–814. https://doi.org/10.1007/s43032-020-00154-1.
O'Shaughnessy, P.J., Monteiro, A., Verhoeven, G., De Gendt, K., Abel, M.H., 2010. Effect of FSH on testicular morphology and spermatogenesis in gonadotrophin-deficient hypogonadal mice lacking androgen receptors. Reproduction 139, 177–184. https://doi.org/10.1530/REP-09-0377.
Paris, L., Peghaire, E., Moné, A., Diogon, M., Debroas, D., Delbac, F., El Alaoui, H., 2020. Honeybee gut microbiota dysbiosis in pesticide/parasite co-exposures is mainly induced by Nosema ceranae. J. Invertebr. Pathol. 172, 107348 https://doi.org/10.1016/j.jip.2020.107348.
Peretz, J., Vrooman, L., Ricke, W.A., Hunt, P.A., Ehrlich, S., Hauser, R., Padmanabhan, V., Taylor, H.S., Swan, S.H., VandeVoort, C.A., Flaws, J.A., 2014. Bisphenol a and reproductive health: update of experimental and human evidence, 2007-2013. Environ. Health Perspect. 122, 775–786. https://doi.org/10.1289/ehp.1307728.
Poling, M.C., Kauffman, A.S., 2013. Organizational and activational effects of sex steroids on kisspeptin neuron development. Front. Neuroendocrin. 34, 3–17. https://doi.org/10.1016/j.yfrne.2012.06.001.
Qiu, L., Chen, M., Wang, X., Qin, X., Chen, S., Qian, Y., Liu, Z., Cao, Q., Ying, Z., 2018. Exposure to concentrated ambient PM2.5 compromises spermatogenesis in a mouse model: Role of suppression of hypothalamus-pituitary-gonads axis. Toxicol. Sci. 162, 318–326. https://doi.org/10.1093/toxsci/kfx261.
Rahman, M.S., Pang, M., 2019. Understanding the molecular mechanisms of bisphenol A action in spermatozoa. Clin. Exp. Reprod. Med. 46, 99–106. https://doi.org/10.5653/cerm.2019.00276.
Riera, M.F., Regueira, M., Galardo, M.N., Pellizzari, E.H., Meroni, S.B., Cigorraga, S.B., 2012R. Signal transduction pathways in FSH regulation of rat Sertoli cell proliferation. Am. J. Physiol. Endocrinol. Metab. 302, E914–E923. https://doi.org/10.1152/ajpendo.00477.2011.
Rizzetto, L., Fava, F., Tuohy, K.M., Selmi, C., 2018. Connecting the immune system, systemic chronic inflammation and the gut microbiome: the role of sex. J. Autoimmun. 92, 12–34. https://doi.org/10.1016/j.jaut.2018.05.008.
Sharma, P., Ghanghas, P., Kaushal, N., Kaur, J., Kaur, P., 2019. Epigenetics and oxidative stress: a twin-edged sword in spermatogenesis. Andrologia 51, e13432. https://doi.org/10.1111/and.13432.
Singh, R.P., Shafeeque, C.M., Sharma, S.K., Pandey, N.K., Singh, R., Mohan, J., Kolluri, G., Saxena, M., Sharma, B., Sastry, K.V.H., Kataria, J.M., Azeez, P.A., 2015. Bisphenol A reduces fertilizing ability and motility by compromising mitochondrial function of sperm. Environ. Toxicol. Chem. 34, 1617–1622. https://doi.org/10.1002/etc.2957.
Spaziani, M., Tarantino, C., Tahani, N., Gianfrilli, D., Sbardella, E., Lenzi, A., Radicioni, A.F., 2021. Hypothalamo-Pituitary axis and puberty. Mol. Cell. Endocrinol. 520, 111094 https://doi.org/10.1016/j.mce.2020.111094.
Vandenberg, L.N., Maffini, M.V., Sonnenschein, C., Rubin, B.S., Soto, A.M., 2009. Bisphenol-A and the great divide: a review of controversies in the field of endocrine disruption. Endocr. Rev. 30, 75–95. https://doi.org/10.1210/er.2008-0021.
Wang, P., Luo, C., Li, Q., Chen, S., Hu, Y., 2014. Mitochondrion-mediated apoptosis is involved in reproductive damage caused by BPA in male rats. Environ. Toxicol. Pharmacol. 38, 1025–1033. https://doi.org/10.1016/j.etap.2014.10.018.
Wang, Y., Rui, M., Nie, Y., Lu, G., 2018. Influence of gastrointestinal tract on metabolism of bisphenol A as determined by in vitro simulated system. J. Hazard. Mater. 355, 111–118. https://doi.org/10.1016/j.jhazmat.2018.05.011.
Wu, Y., Ma, J., Sun, Y., Tang, M., Kong, L., 2020. Effect and mechanism of PI3K/AKT/mTOR signaling pathway in the apoptosis of GC-1 cells induced by nickel nanoparticles. Chemosphere 255, 126913. https://doi.org/10.1016/j.chemosphere.2020.126913.
Xi, W., Lee, C.K., Yeung, W.S., Giesy, J.P., Wong, M.H., Zhang, X., Hecker, M., Wong, C. K., 2011. Effect of perinatal and postnatal bisphenol A exposure to the regulatory circuits at the hypothalamus-pituitary-gonadal axis of CD-1 mice. Reprod. Toxicol. 31, 409–417. https://doi.org/10.1016/j.reprotox.2010.12.002.
Xie, M., Bu, P., Li, F., Lan, S., Wu, H., Yuan, L., Wang, Y., 2016. Neonatal bisphenol A exposure induces meiotic arrest and apoptosis of spermatogenic cells. Oncotarget 7, 10606–10615. https://doi.org/10.18632/oncotarget.7218.
Xu, H., Shen, L., Chen, X., Ding, Y., He, J., Zhu, J., Wang, Y., Liu, X., 2016. mTOR/P70S6K promotes spermatogonia proliferation and spermatogenesis in Sprague Dawley rats. Reprod. Biomed. Online 32, 207–217. https://doi.org/10.1016/j.rbmo.2015.11.007.
Zhan, J., Ma, X., Liu, D., Liang, Y., Li, P., Cui, J., Zhou, Z., Wang, P., 2020. Gut microbiome alterations induced by tributyltin exposure are associated with

increased body weight, impaired glucose and insulin homeostasis and endocrine disruption in mice. Environ. Pollut. 266, 115276 https://doi.org/10.1016/j.envpol.2020.115276.

Zhang, J., Yao, Y., Pan, J., Guo, X., Han, X., Zhou, J., Meng, X., 2020. Maternal exposure to di-(2-ethylhexyl) phthalate (DEHP) activates the PI3K/Akt/mTOR signaling pathway in F1 and F2 generation adult mouse testis. Exp. Cell Res. 394, 112151 https://doi.org/10.1016/j.yexcr.2020.112151.

Zhang, M., Jiang, M., Bi, Y., Zhu, H., Zhou, Z., Sha, J., 2012. Autophagy and apoptosis act as partners to induce germ cell death after heat stress in mice. PLoS One 7, e41412. https://doi.org/10.1371/journal.pone.0041412.

Zhao, T., Wei, Y., Wang, J., Han, L., Sun, M., Wu, Y., Shen, L., Long, C., Wu, S., Wei, G., 2020. The gut-microbiota-testis axis mediated by the activation of the Nrf2 antioxidant pathway is related to prepuberal steroidogenesis disorders induced by di-(2-ethylhexyl) phthalate. Environ. Sci. Pollut. Res. Int. 27, 35261–35271. https://doi.org/10.1007/s11356-020-09854-2.

Zhao, T., Tang, X., Li, D., Zhao, J., Zhou, R., Shu, F., Jia, W., Fu, W., Xia, H., Liu, G., 2022. Prenatal exposure to environmentally relevant levels of PBDE-99 leads to testicular dysgenesis with steroidogenesis disorders. J. Hazard. Mater. 424, 127547 https://doi.org/10.1016/j.jhazmat.2021.127547.

Abbara, A, Clarke, S.A., Dhillo, W.S, 2021. Clinical Potential of Kisspeptin in Reproductive Health. Trends. Mol. Med. 27, 807–823. https://doi.org/10.1016/j.molmed.2021.05.008.